sciendo

CIVIL AND ENVIRONMENTAL ENGINEERING REPORTS

E-ISSN 2450-8594

CEER 2021; 31 (3): 0152-0176
DOI: 10.2478/ceer-2021-0039
*Original Research Article*

# PRESSURE SETTLEMENT BEHAVIOUR AND BEARING CAPACITY OF ASYMMETRIC EMBEDDED PLUS SHAPED FOOTING ON LAYERED SAND

Priyanka RAWAT[1], Rakesh Kumar DUTTA[2]
[1]PG Student, Department of Civil Engineering, National Institute of Technology, Hamirpur, India
[2]Professor, Department of Civil Engineering, National Institute of Technology, Hamirpur, India

A b s t r a c t

The aim of the present numerical study was to analyse the pressure settlement behaviour and bearing capacity of asymmetric plus shaped footing resting on loose sand overlying dense sand at varying embedment depth. The numerical investigation was carried out using ABAQUS software. The effect of depth of embedment, friction angle of upper loose and lower dense sand layer and thickness of upper loose sand on the bearing capacity of the asymmetric plus shaped footing was studied in this investigation. Further, the comparison of the results of the bearing capacity was made between the asymmetric and symmetric plus shaped footing. The results reveal that with increase in depth of embedment, the dimensionless bearing capacity of the footings increased. The highest increase in the dimensionless bearing capacity was observed at embedment ratio of 1.5. The increase in the bearing capacity was 12.62 and 11.40 times with respect to the surface footings F1 and F2 corresponding to a thickness ratio of 1.5. The lowest increase in the dimensionless bearing capacity was observed at embedment ratio of 0.1 and the corresponding increase in the bearing capacity was 1.05 and 1.02 times with respect to the surface footing for footings F1 and F2 at a thickness ratio of 1.5.

[1] Corresponding author: PG Student, Department of Civil Engineering, National Institute of Technology, Hamirpur, India, e-mail: 19m101@nith.ac.in

Keywords: asymmetric plus shaped footing, symmetric plus shaped footing, embedment depth, ultimate bearing capacity, friction angle, thickness of upper layer, layered sand

## 1. INTRODUCTION

The demand for multi-story buildings with an asymmetric plan has increased as a result of a shortage of construction land in metropolitan areas. For both economic and aesthetic purposes, asymmetric plan shaped designs are preferred these days. Such designs require asymmetric plan shaped footings. There are studies on the bearing capacity of asymmetric or symmetric plan shaped footings in the literature that indicate that the performance of such footings (plus, H and T) was comparable to that of a square footing having similar area and lying on single layer of sand [6,7,3]. Research conducted on circular footing reveals that the performance of embedded circular footing is superior to that of the surface circular footing [12]. Further, it has been found from the literature [9], that the ultimate bearing capacity increased with the increase in the depth to width ratio of the strip footing. The effect of embedment depth on the bearing capacity of the strip footing was investigated in the literature, and it was reported that bearing capacity factors were dependent on internal angle of friction and embedment depth. The bearing capacity of a footing with a higher friction angle and embedment depth was also higher [14]. For a given value of angle of friction, the degree of embedment affects the bearing capacity of the footing [18]. As a result, it was reported that as embedment depth increases, ultimate bearing capacity also increases [1,134,18] and the rate of increase in ultimate bearing capacity tends to a limiting value [1]. According to a study on strip and circular footings resting on loose sand overlying dense sand [9,13], the bearing capacity factors for the footing on layered sand was dependent on the relative strength of both the layer and the thickness of the upper layer below the base of the footing [9] and the influence of upper layer thickness depends mainly on shear strength parameters and ratio of bearing capacity of the layers [13]. It is evident from the above studies that no study was conducted so far for the asymmetric plus plan shaped footing resting on loose sand overlying dense sand. In order to fill this research gap, in the present paper an attempt has been made to conduct a numerical study to understand the pressure settlement behaviour of embedded asymmetric plus plan shaped footing resting on layered sand (loose over dense). The results obtained from this numerical study were compared with the results of symmetric plus shaped footing. The parameters varied were angle of friction of both layers, thickness of upper loose sand layer and depth of embedment.

## 2. PROBLEM DOMAIN AND MODELLING PARAMETERS

A numerical study was conducted on asymmetric plus plan shaped footing (designated as F1, Fig. 1(a)) and symmetric plus plan shaped footing (designated as F2, Fig. 1(b)) resting on loose sand (designated as S1) overlying dense sand (designated as S2). The F1 and F2 footings were made out of the square footing of size 2.0 m x 2.0 m as shown in Fig. 1.

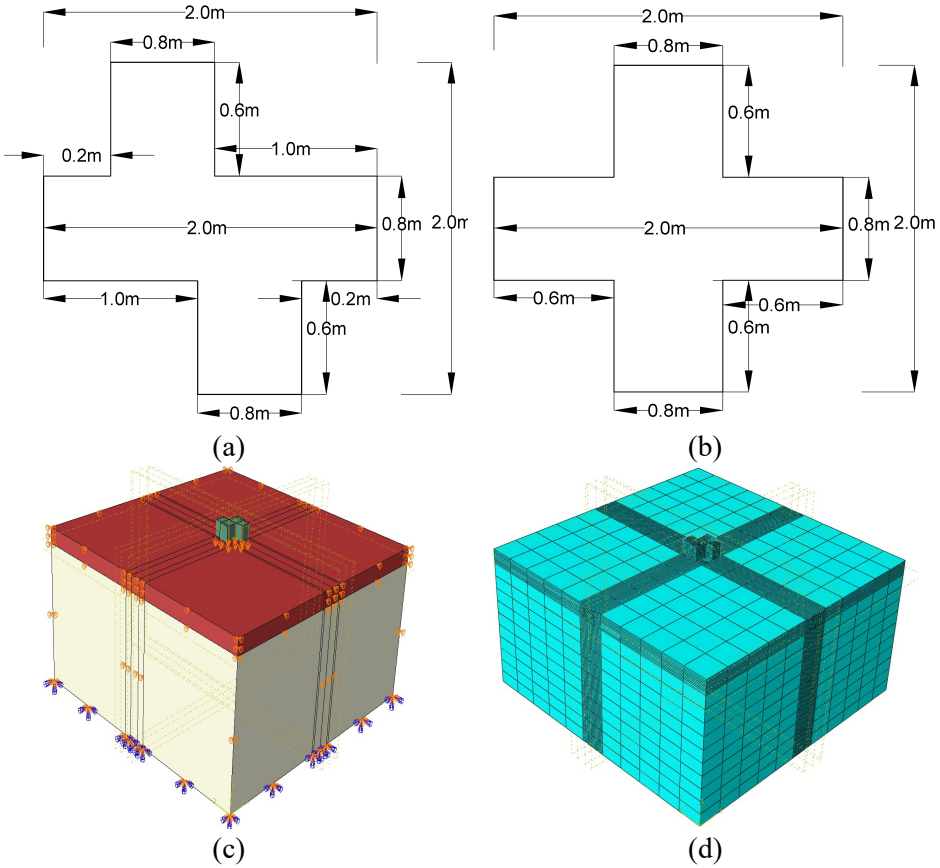


Fig. 1. Plan view of footing (a) F1 (b) F2 (c) problem domain and boundary conditions applied (d) meshing for footing F1 at $D_f/B=0$ on layered sand

The embedment depth to width ratio ($D_f/B$) was varied from 0 to 1.5. The thickness of both the footing was chosen as 1 m. The footings were considered made of concrete of M25 grade having a characteristic compressive strength equal to 25 N/mm$^2$ (equivalent to C25). Numerical study for the both the footings was conducted under vertical load. Geostatic stress was applied prior to application of

the vertical load. The thickness of sand S1 was varied from 0.5B to 1.5B while the thickness of sand S2 was considered as of infinite depth. The friction angle of the sand S1 ($\phi_1$) and S2 ($\phi_2$) was varied from 30º to 34º and 40º to 44º respectively at an interval of 2º. The unit weight of sand S1 ($\gamma_1$) and S2 ($\gamma_2$) were taken corresponding to the considered angle of friction [2]. The unit weights used for modelling were tabulated in Table 1.

Table 1. Unit weight of sand corresponding to the friction angle as per [4]

| Unit weight (kN/m$^3$) | Friction angle |
|---|---|
| 13.5 | 30º |
| 14.5 | 32º |
| 15 | 34º |
| 17.5 | 40º |
| 18 | 42º |
| 19 | 44º |

The Poisson's ratio for the sand S1 ($\mu_1$) and sand S2 ($\mu_2$) were taken as 0.3 and 0.34 respectively as per [2]. The modulus of elasticity for the sand S1 ($E_1$) and S2 ($E_2$) were 20 MPa and 65 MPa respectively as per [2]. The dilation angle for the sand S1 and S2 for the modelling was calculated using the formula $\phi$ -30 [16].

## 3. MESHING, BOUNDARY CONDITION AND SOFTWARE VALIDATION

A 3D finite element analysis was performed using ABAQUS. For modelling, the dimensions of the model were chosen as 10B along length, 10B along width and 5B along depth in order to ensure that the model boundaries do not interfere [19]. The boundary condition was applied to all the four side faces of the soil in such a way that their horizontal movement was restricted and base of the soil was kept fixed. For modelling Mohr Coulomb model was used as it requires less computational time in comparison to other soil hardening models [17]. Fig. 1(c) shows the problem domain and boundary conditions. For meshing, C3D8R element was used. Meshing was done in such a way that it was finer closer to the centre of the footing and coarser when moved away from the centre of the footing. The complete meshing scheme is shown in Fig. 1(d).

### 3.1 Software Validation

Prior to the analysis, it was thought to validate the software with the experimental results reported on the symmetric plus shaped footing resting on single layer of sand in literature [8]. For validation, the sand friction angle and the interface friction angle between the sand and the footing were 36.06°, 38.64°, 39.86°, 41.72° and 36.46°, 38.07°, 39.03° and 40.66°, respectively, for relative densities of 30 %, 40 %, 50 %, and 60 %. The sand had a dry unit weight of 14.09kN/m$^{3,}$

14.37 kN/m$^3$ , 14.66 kN/m$^3$ and 14.96 kN/m$^3$ corresponding to a relative densities of 30 %, 40 %, 50 %, and 60 % respectively. The dimension of sand model considered was 700 mm × 450 mm × 600 mm. The symmetric plus shaped footing was made out of a square footing of width 80 mm. The flange width of the footing and the thickness was 26 mm and 10 mm respectively. The elastic modulus of the sand was calculated using 1200(N+6) as per **[5],** where N is standard penetration number which was calculated using a correlation between angle of friction and N as per **[15].** The poison's ratio of the sand was considered as 0.3 as per [2]. The density (γ), modulus of elasticity (E) and the Poisson ratio (υ) of the steel footing was taken as 78.5 kN/m$^3$, 210 GPa and 0.303 respectively as per **[11].** The comparison of the results was shown in Table 2. Table 2 shows that at various relative densities, the average deviation in bearing capacity was around 11.32 %. This discrepancy in the results can be due to the use of empirical correlation in determining sand modelling parameters.

Table 2. Comparison of results for software validation

| Relative density R.D. (%) | Bearing capacity ($q_u$) at s/B ratio of 10% | |
|---|---|---|
| | Gnananandarao et al [8] | Present work |
| 30 | 91.43 | 94.268 |
| 40 | 160 | 151.20 |
| 50 | 210.57 | 208.67 |
| 60 | 270.00 | 302.32 |

## 4. RESULT AND DISCUSSION

Figures 2 and 3 show the pressure settlement plots obtained from the numerical study at H= 0.5B and corresponding to different sand (S1 and S2) friction angle combinations for the footings F1 and F2. The bearing pressure was obtained by taking the minimum of peak pressure or pressure corresponding to the s/B ratio of 5%, whichever occur earlier as per [12]. If the peak is not clearly observed, then double tangent method was used to calculate the same. Study of Fig. 2(a) reveals that with increase in embedment depth to width ratio, the pressure-settlement behaviour changed from local shear to general shear failure. Further, from Fig. 2(a), at H/B equal to 0.5, the change in the behaviour from local to general was observed at a $D_f/B$ ratio ≥ 0.5. Similarly, for H/B equal to 1.0, the change in the behaviour was observed at $D_f/B \geq 1.0$. Similar trend was observed corresponding to all combination of friction angle considered as evident from Fig.2.

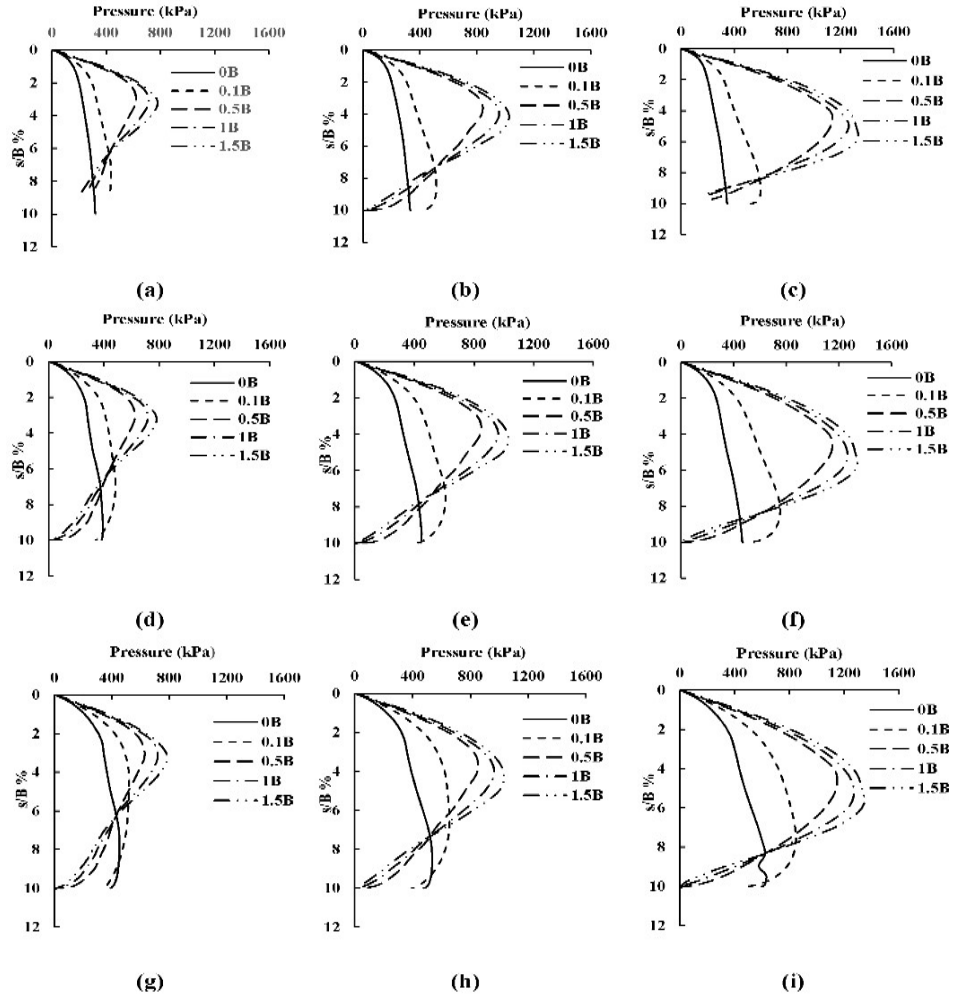


Fig. 2. Pressure settlement ratio curve for the footing F1 at a H/B =0.5 for different combinations of friction angles ($\emptyset_1$; $\emptyset_2$) of sand S1 and S2 (a) 30°; 40° (b) 30°; 42° (c) 30°; 44° (d) 32°; 40° (e) 32°; 42° (f) 32°; 44° (g) 34°; 40° (h) 34°; 42° (i) 34°; 44°

The above stated behaviour in case of footing F2 was observed at all H/B and $D_f$/B ratios and was attributed to the involvement of larger participation of sand S2 with the increase in the depth of embedment. Study of Fig. 3(a) reveals that a clear peak was observed at all depth of embedment considered, which indicate that a general shear failure was observed in case of footing F2. This observation confirms the findings reported in literature [8]. Similar trend was observed corresponding to all combination of friction angle considered as evident from Fig. 3.

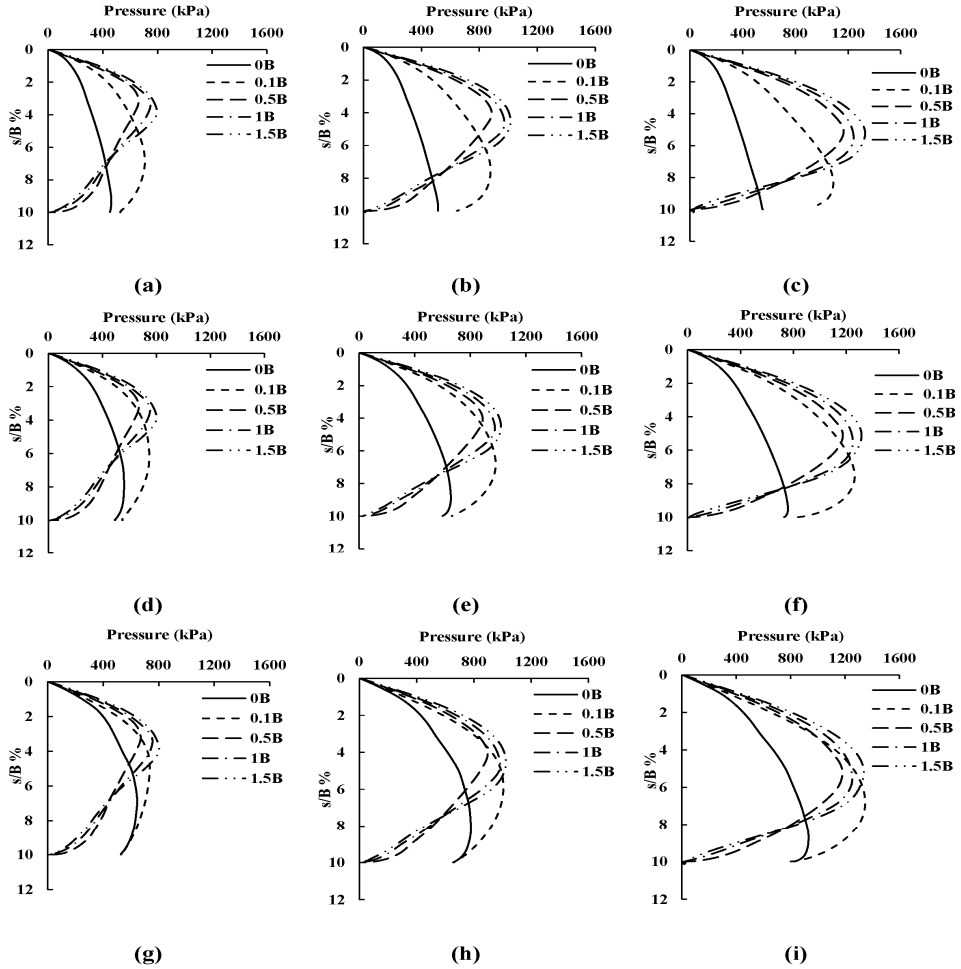


Fig. 3. Pressure settlement ratio curve for the footing F2 at a H/B =0.5 for different $D_f$/B ratio and combinations of friction angles ($\emptyset_1$; $\emptyset_2$) of sand S1 and S2 (a) 30°; 40° (b) 30°; 42° (c) 30°; 44° (d) 32°; 40° (e) 32°; 42° (f) 32°; 44° (g) 34°; 40° (h) 34°; 42° (i) 34°; 44°

Further examination of Figs 2 and 3 reveals that there are two values of s/B at pressure = 0. Beyond the peak values, this second value is seen. It should be emphasised that the pressure settlement behaviour beyond peak values was not the subject of the current study, which would necessitate a more in-depth investigation to determine the reasons for the post-peak behaviour.

### 4.1 Effect of Depth of Embedment on Bearing Capacity

In order to study the effect of depth of embedment on the dimensionless bearing capacity ($q_u/\gamma_1 B$) at varying $D_f$/B ratio for the footings F1 and F2 corresponding to H/B ratios of 0.5, 1 and 1.5, the curves were shown in Fig. 4, Fig. 5 and Fig. 6 respectively. The dimensionless bearing capacity was tabulated in Table 3, Table 4 and Table 5 respectively. Study of Table 3 reveals that with the increase in the depth of embedment, the dimensionless bearing capacity increased up to a $D_f$/B ratio of 0.5 and beyond this, the increase in the dimensionless bearing capacity was marginal. Further, on comparison of Fig. 4(a) and Fig. 4(b), it was observed that at a $D_f$/B equal to 0.1, the dimensionless bearing capacity for the footing F2 was higher than that of F1. When the depth of embedment to width ratio increased from 0.5 to 1.5, the difference in the dimensional bearing capacity of both the footing reduced and reached to almost similar value. This could be attributed the extension of failure surfaces to deeper dense sand S2 bringing the difference in the dimensionless bearing capacity for both the footings to almost negligible. Similar trend in the dimensionless bearing capacity was observed for other combinations as evident from Fig. 5 and Fig. 6.

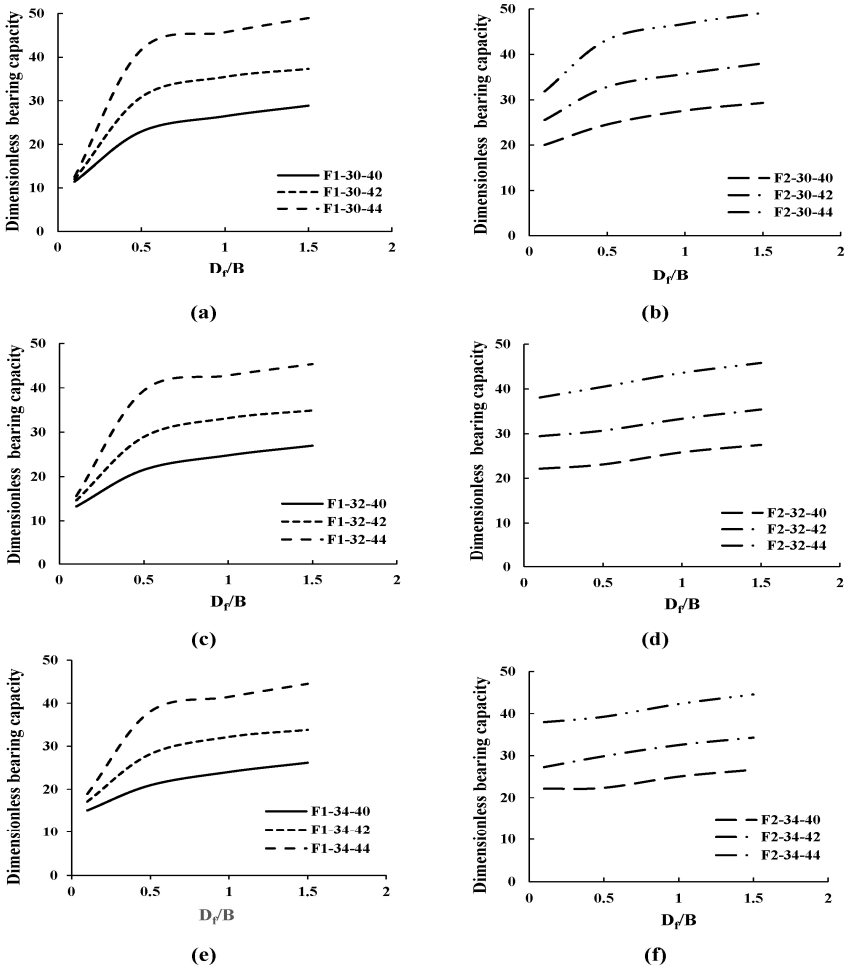


Fig. 4. Variation of dimensionless bearing capacity with $D_f/B$ ratio at H/B=0.5 for Ø1 = 30° (a,b), 32° (c,d) and 34° (e,f) for the footing F1 (a,c,e) and F2 (b,d,f)

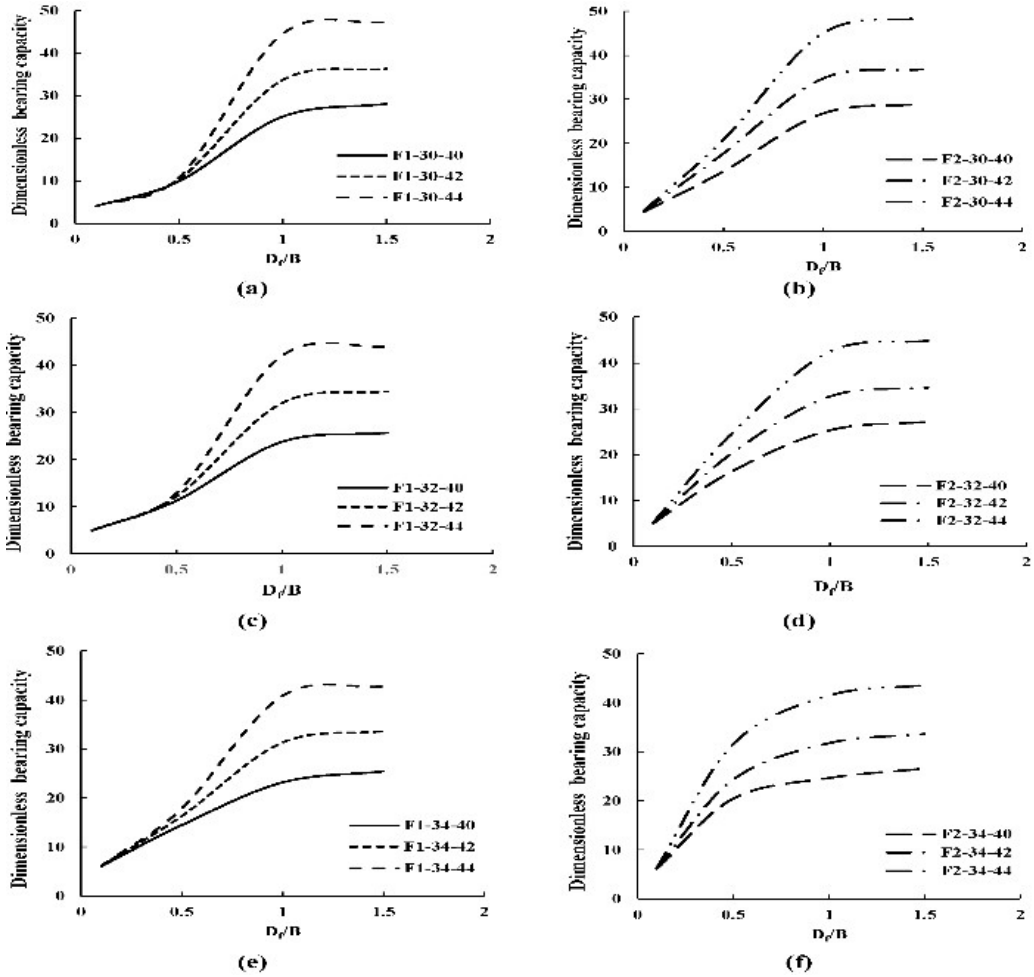


Fig. 5. Variation of dimensionless bearing capacity with $D_f/B$ ratio at H/B=1 for ∅1 = 30° (a,b), 32° (c,d) and 34° (e,f) for the footing F1 (a,c,e) and F2 (b,d,f)

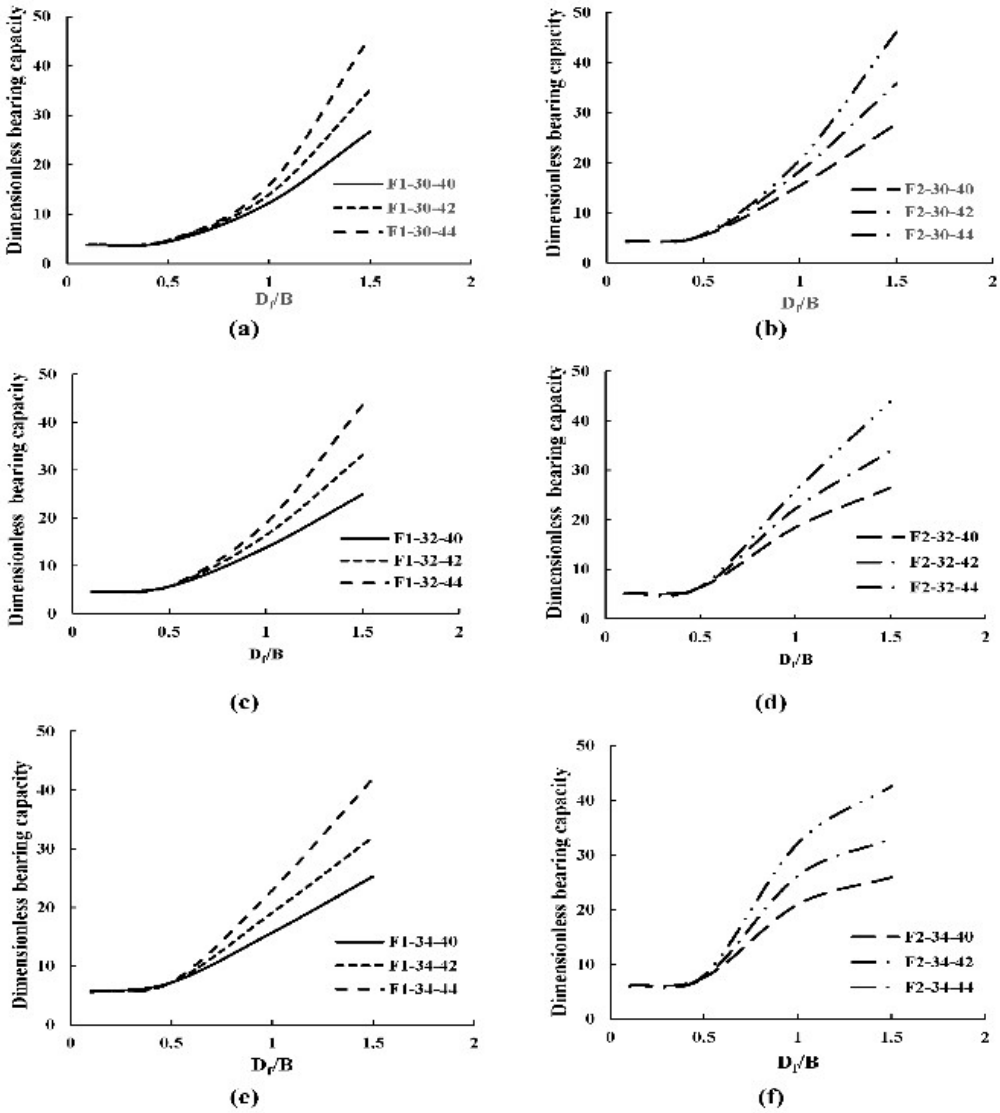


Fig. 6. Variation of dimensionless bearing capacity with $D_f/B$ ratio at H/B=1.5 for Ø1 = 30° (a,b), 32° (c,d) and 34° (e,f) for the footing F1 (a,c,e) and F2 (b,d,f)

Table 3. Dimensionless bearing capacity of footing F1 and F2 at H/B =0.5

| Dimensionless bearing capacity ($q_u/\gamma_1 B$) | | | | | |
|---|---|---|---|---|---|
| H/B Ratio | $\emptyset_1$ | $\emptyset_2$ | $D_f/B$ | F1 | F2 |
| 0.5 | 30° | 40° | 0 | 8.37 | 12.05 |
| | | | 0.1 | 11.44 | 20.04 |
| | | | 0.5 | 22.94 | 24.54 |
| | | | 1 | 26.45 | 27.62 |
| | | | 1.5 | 28.87 | 29.31 |
| | | 42° | 0 | 8.61 | 12.53 |
| | | | 0.1 | 11.99 | 25.54 |
| | | | 0.5 | 30.84 | 32.81 |
| | | | 1 | 35.46 | 35.71 |
| | | | 1.5 | 37.31 | 38.03 |
| | | 44° | 0 | 9.24 | 12.59 |
| | | | 0.1 | 12.52 | 31.86 |
| | | | 0.5 | 41.70 | 43.22 |
| | | | 1 | 45.70 | 46.75 |
| | | | 1.5 | 48.98 | 49.18 |
| | 32° | 40° | 0 | 8.12 | 15.54 |
| | | | 0.1 | 13.24 | 22.15 |
| | | | 0.5 | 21.51 | 23.12 |
| | | | 1 | 24.77 | 25.82 |
| | | | 1.5 | 26.96 | 27.49 |
| | | 42° | 0 | 8.54 | 16.84 |
| | | | 0.1 | 14.61 | 29.44 |
| | | | 0.5 | 28.92 | 30.68 |
| | | | 1 | 33.17 | 33.33 |
| | | | 1.5 | 34.90 | 35.41 |
| | | 44° | 0 | 9.64 | 17.55 |
| | | | 0.1 | 15.61 | 38.09 |
| | | | 0.5 | 39.37 | 40.49 |
| | | | 1 | 42.80 | 43.59 |
| | | | 1.5 | 45.37 | 45.83 |
| | 34° | 40° | 0 | 9.21 | 18.09 |
| | | | 0.1 | 15.08 | 22.14 |
| | | | 0.5 | 20.93 | 22.36 |
| | | | 1 | 24.03 | 25.01 |
| | | | 1.5 | 26.17 | 26.66 |
| | | 42° | 0 | 9.84 | 20.72 |
| | | | 0.1 | 17.15 | 27.28 |
| | | | 0.5 | 28.17 | 29.87 |
| | | | 1 | 32.17 | 32.53 |
| | | | 1.5 | 33.80 | 34.29 |
| | | 44° | 0 | 10.31 | 22.60 |
| | | | 0.1 | 18.91 | 37.97 |
| | | | 0.5 | 38.06 | 39.26 |
| | | | 1 | 41.48 | 42.29 |
| | | | 1.5 | 44.51 | 44.56 |

Table 4. Dimensionless bearing capacity of footing F1 and F2 at H/B =1

| Dimensionless bearing capacity ($q_u/\gamma_1 B$) | | | | | |
|---|---|---|---|---|---|
| H/B Ratio | $\emptyset_1$ | $\emptyset_2$ | Df/B | F1 | F2 |
| 1 | 30° | 40° | 0 | 3.65 | 4.33 |
| | | | 0.1 | 4.05 | 4.41 |
| | | | 0.5 | 9.92 | 13.62 |
| | | | 1 | 25.11 | 26.79 |
| | | | 1.5 | 28.15 | 28.93 |
| | | 42° | 0 | 3.65 | 4.39 |
| | | | 0.1 | 4.05 | 4.54 |
| | | | 0.5 | 10.43 | 17.68 |
| | | | 1 | 33.71 | 34.72 |
| | | | 1.5 | 36.40 | 36.82 |
| | | 44° | 0 | 3.80 | 4.58 |
| | | | 0.1 | 4.05 | 4.65 |
| | | | 0.5 | 10.74 | 20.81 |
| | | | 1 | 44.58 | 45.00 |
| | | | 1.5 | 47.38 | 48.55 |
| | 32° | 40° | 0 | 4.24 | 4.95 |
| | | | 0.1 | 4.93 | 5.06 |
| | | | 0.5 | 11.28 | 16.33 |
| | | | 1 | 23.76 | 25.30 |
| | | | 1.5 | 25.69 | 27.16 |
| | | 42° | 0 | 4.28 | 4.96 |
| | | | 0.1 | 4.94 | 5.10 |
| | | | 0.5 | 12.19 | 20.25 |
| | | | 1 | 31.98 | 32.67 |
| | | | 1.5 | 34.47 | 34.61 |
| | | 44° | 0 | 4.30 | 4.97 |
| | | | 0.1 | 4.94 | 5.18 |
| | | | 0.5 | 12.83 | 24.57 |
| | | | 1 | 42.01 | 42.42 |
| | | | 1.5 | 44.01 | 44.84 |
| | 34° | 40° | 0 | 5.26 | 5.88 |
| | | | 0.1 | 6.08 | 6.15 |
| | | | 0.5 | 14.46 | 20.44 |
| | | | 1 | 23.17 | 24.63 |
| | | | 1.5 | 25.43 | 26.56 |
| | | 42° | 0 | 5.35 | 5.94 |
| | | | 0.1 | 6.13 | 6.23 |
| | | | 0.5 | 16.31 | 24.32 |
| | | | 1 | 31.30 | 31.74 |
| | | | 1.5 | 33.62 | 33.63 |
| | | 44° | 0 | 5.40 | 5.98 |
| | | | 0.1 | 6.16 | 6.27 |
| | | | 0.5 | 17.82 | 31.57 |
| | | | 1 | 40.84 | 41.44 |
| | | | 1.5 | 42.77 | 43.58 |

Table 5. Dimensionless bearing capacity of footing F1 and F2 at H/B =1.5

| Dimensionless bearing capacity ($q_u/\gamma_1 B$) | | | | | |
|---|---|---|---|---|---|
| H/B Ratio | $\emptyset_1$ | $\emptyset_2$ | Df/B | F1 | F2 |
| 1.5 | 30° | 40° | 0 | 3.54 | 3.89 |
| | | | 0.1 | 3.76 | 4.19 |
| | | | 0.5 | 4.42 | 5.44 |
| | | | 1 | 12.26 | 15.44 |
| | | | 1.5 | 26.67 | 27.74 |
| | | 42° | 0 | 3.62 | 3.95 |
| | | | 0.1 | 3.79 | 4.25 |
| | | | 0.5 | 4.71 | 5.52 |
| | | | 1 | 13.94 | 18.34 |
| | | | 1.5 | 35.11 | 35.79 |
| | | 44° | 0 | 3.63 | 4.04 |
| | | | 0.1 | 3.81 | 4.39 |
| | | | 0.5 | 4.75 | 5.72 |
| | | | 1 | 15.85 | 20.58 |
| | | | 1.5 | 45.83 | 46.07 |
| | 32° | 40° | 0 | 4.15 | 4.68 |
| | | | 0.1 | 4.51 | 5.05 |
| | | | 0.5 | 5.63 | 6.33 |
| | | | 1 | 13.78 | 18.42 |
| | | | 1.5 | 24.93 | 26.46 |
| | | 42° | 0 | 4.22 | 4.69 |
| | | | 0.1 | 4.56 | 5.06 |
| | | | 0.5 | 5.68 | 6.37 |
| | | | 1 | 16.37 | 22.19 |
| | | | 1.5 | 33.13 | 33.84 |
| | | 44° | 0 | 4.24 | 4.70 |
| | | | 0.1 | 4.57 | 5.06 |
| | | | 0.5 | 5.70 | 6.43 |
| | | | 1 | 18.92 | 25.81 |
| | | | 1.5 | 43.61 | 43.89 |
| | 34° | 40° | 0 | 5.15 | 5.63 |
| | | | 0.1 | 5.54 | 6.06 |
| | | | 0.5 | 7.20 | 7.60 |
| | | | 1 | 15.71 | 20.96 |
| | | | 1.5 | 25.27 | 25.92 |
| | | 42° | 0 | 5.27 | 5.92 |
| | | | 0.1 | 5.71 | 6.07 |
| | | | 0.5 | 7.20 | 7.63 |
| | | | 1 | 19.10 | 26.18 |
| | | | 1.5 | 32.01 | 32.98 |
| | | 44° | 0 | 5.29 | 5.92 |
| | | | 0.1 | 5.72 | 6.12 |
| | | | 0.5 | 7.28 | 8.03 |
| | | | 1 | 22.93 | 32.10 |
| | | | 1.5 | 41.98 | 42.56 |

### 4.2. Effect of Friction Angle of S1 and S2 on Bearing Capacity

In order to observe the effect of friction angle of sand S1 and S2 on the bearing capacity, the typical pressure settlement ratio plots corresponding to $D_f/B$ of 0 and 0.5 and at H/B ratio of 0.5, 1 and 1.5 were shown in Fig. 7 and Fig. 8 respectively.

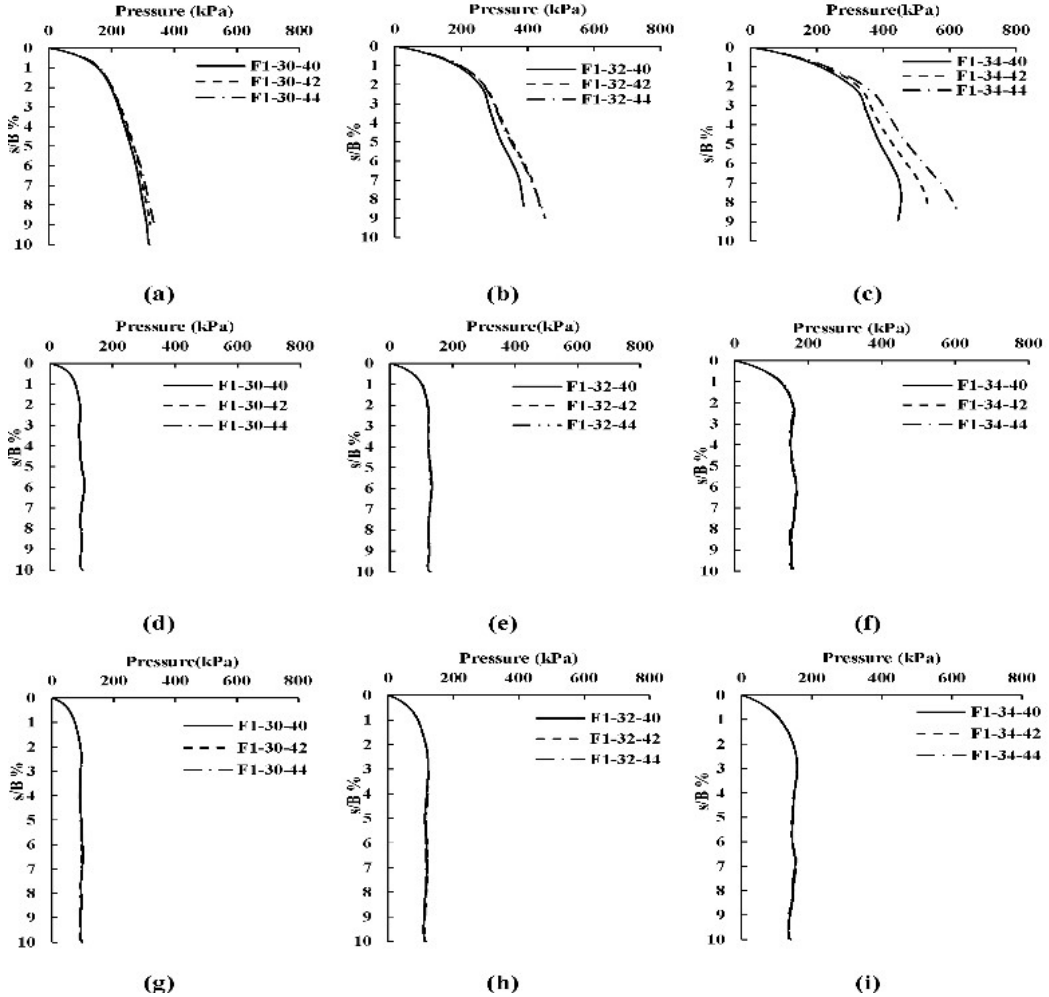


Fig. 7. Pressure settlement ratio plot at $D_f/B=0$ for the footing (F1) at H/B ratio of (a, b, c) 0.5 (d,e,f) 1 (g,h,i) 1.5

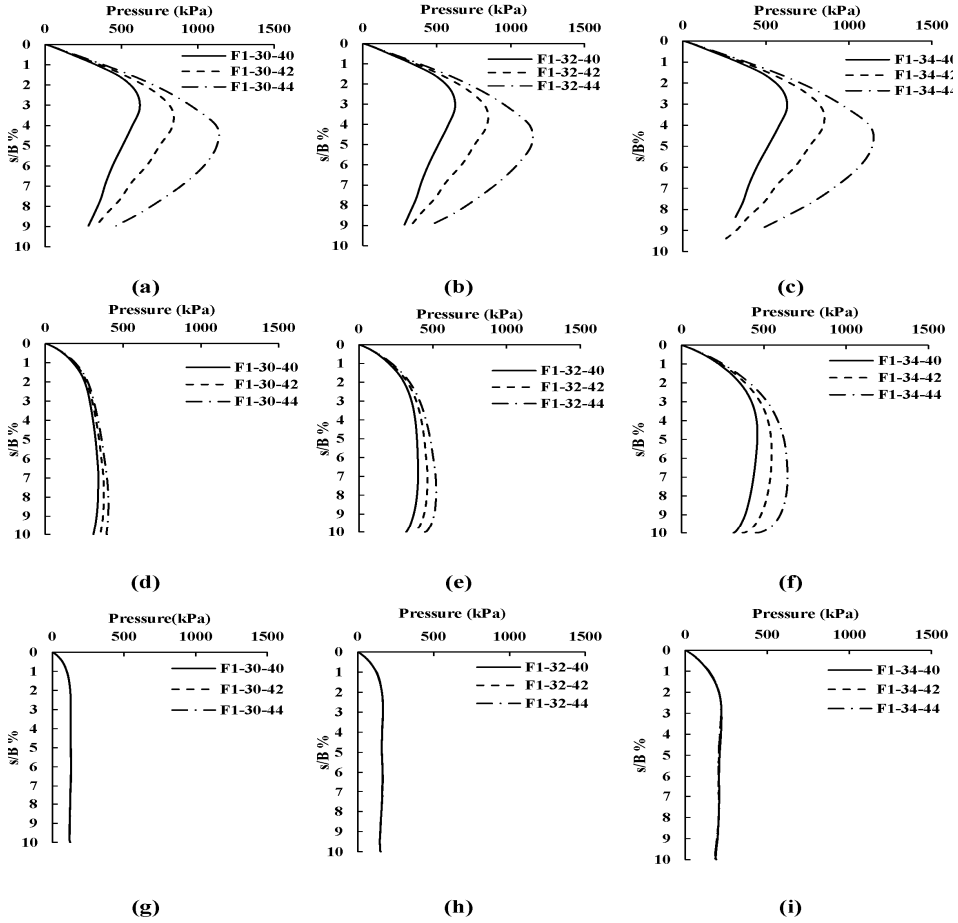


Fig.8. Pressure settlement ratio plot at $D_f/B$=0.5 for the footing (F1) at H/B ratio of (a, b, c) 0.5 (d,e,f) 1 (g,h,i) 1.5

Study of Fig. 7(a) to Fig. 7(c) reveals that with increase in friction angle of sand S1 and S2, the bearing capacity increased and the effect of friction angle of sand S2 was higher at larger values of friction angle of sand S1. Further, study of Fig. 7(d) to Fig. 7(i) shows that as the depth of sand S1 increased, the effect of friction angle of sand S2 on the bearing capacity was marginal while the effect of friction angle of sand S1 was significant. Study of Fig. 8(a) to Fig.8(f), at a $D_f/B$=0.5, the effect of friction angles of sand S1 and S2 was similar to that as shown in Fig. 8(a) to Fig. 8(c). The effect of friction angle of sand S2 was marginal at H/B = 1.5 as evident from Fig 8. (g) to Fig. 8(i). Hence, from the above, it was concluded that as failure surface approached sand S2, the effect of friction angles of sand S2 and S1was higher and lower respectively. This was due to the fact that footing

with a deeper embedment and a higher friction angle would have a higher bearing capacity [14].

### 4.3. Effect of Thickness of Upper Loose Sand on Bearing Capacity

In order to study the effect of thickness of upper sand layer on the behaviour of footing F1 and F2, the results were plotted in Fig. 9 (a) to Fig. 9 (e). For this purpose, the thickness ratio and depth ratio was varied from 0.5 to 1.5 and 0 to 1.5 respectively.

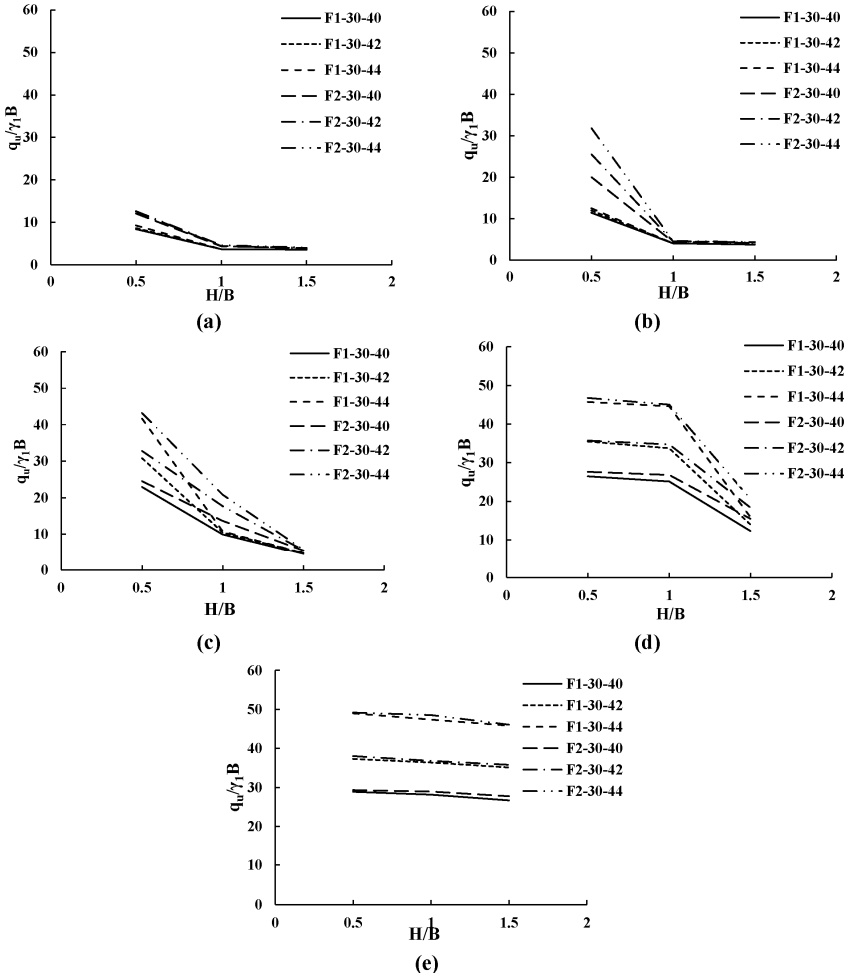


Fig. 9. Variation of dimensionless bearing capacity with H/B ratio for $D_f/B$ (a) 0 (b) 0.1 (c) 0.5 (d) 1 (e) 1.5

Study of Fig 9(a) reveals that with the increase in the thickness of sand S1, the dimensionless bearing capacity decreased for the footings F1 and F2. This was

due to the fact that the bearing capacity primarily depends on the relative strength of both the layer as well as depth of upper sand layer below the base of footing [9]. As the depth of upper loose sand layer increases, the contribution towards the bearing capacity of the lower dense sand layer decreases. Similar trend of reduction in the dimensionless bearing capacity with the increase in H/B ratio was observed from Fig. 9(b) to Fig. 9(e). Further, from Fig. 9(e), the reduction in the dimensionless bearing capacity was marginal at $D_f$/B ratio of 1.5.

### 4.3.1. Comparison

Comparison of the dimensionless bearing capacity for the footings F1 and F2 having similar area was attempted and the results were plotted in Fig. 9. Study of Fig. 9(a) reveals that at an H/B ratio of 0.5, the dimensionless bearing capacity of the footing F2 was higher in comparison to the footing F1. This could be due to lesser interference of heterogeneous shear zones beneath the footing F1 in comparison to footing F2. This lesser interference in the case of footing F1 could be due to a lack of adequate distance between its flanges at two diagonally opposite corners, while the distance between the flanges at the other two diagonally opposite corners was greater than the required, resulting in an overall reduction in bearing capacity. However, further investigations are required to verify this aspect. Further, study of Fig.9 (a) reveals that as the H/B ratio increased the difference between dimensionless bearing capacities of both the footing decreased and found to be almost same at an H/B ratio of 1.5. This may be due to the fact that at higher H/B ratios, the impact of sand S2 diminishes and a homogenous sand condition beneath the footing prevails. The study of Fig. 9(a) to Fig. 9(e) further reveals that the embedment depth has significant effect on dimensionless bearing capacity of footing F1 and F2. For example, with the increase in the embedment depth, the dimensionless bearing capacity of the footings F1 and F2 was found to be similar for the cases (1) H/B = 0.5 with $D_f$/B> 0.5, (2) H/B = 1 with $D_f$/B≠ 0.5 and (3) H/B = 1.5 with $D_f$/B≠ 1. In all the above cases, the influence of either sand S1 or S2 prevails below the base of the footing. The above results were in agreement with the previous findings [3].

### 4.4. Displacement Contours

Typical displacement contours for Footing F1 and F2 with varying $D_f$/B ratio ranging from 0 to 1.5 corresponding to H/B ratio of 0.5 and at a constant friction angle of the upper loose sand (30º) and lower dense sand (40º) layer was presented in Figure 10.

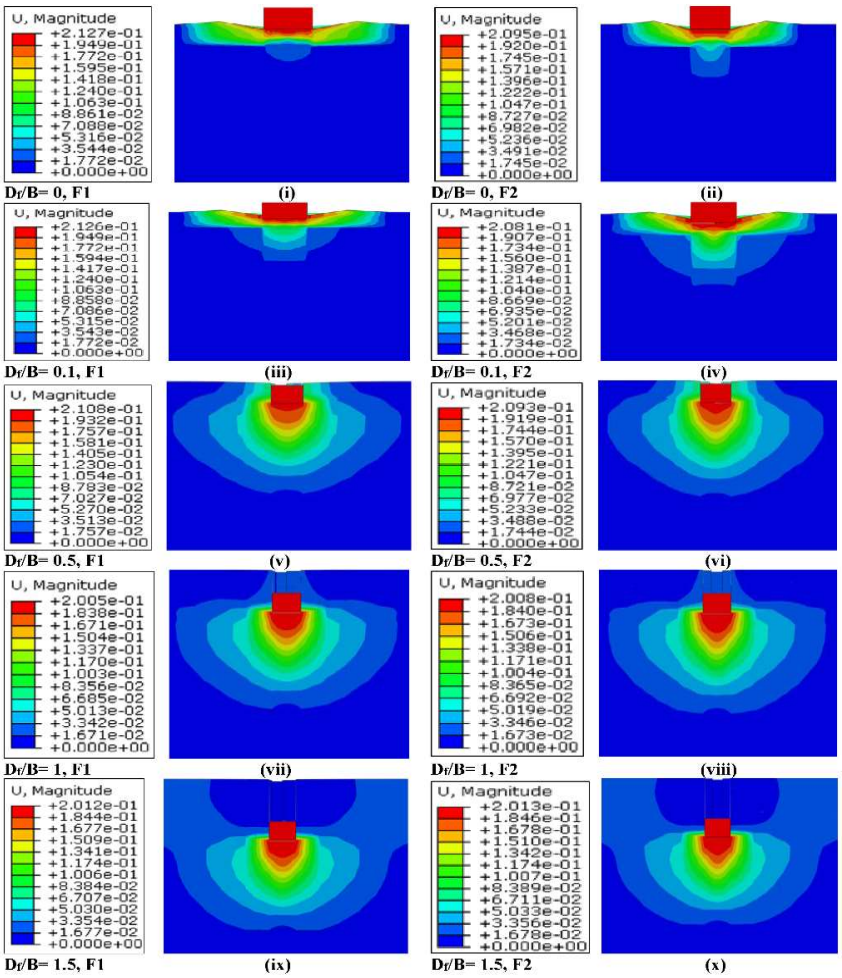


Fig. 10. Typical displacement contours at H/B=0.5 with different $D_f/B$ ratio corresponding to $\emptyset_1 = 30°$ and $\emptyset_2 = 40°$ for footing F1 (i, iii, v, vii, ix) and F2 (ii, iv, vi, viii, x)

A close examination of Fig.10 (i) and Fig.10 (ii) reveals that there was no difference in the extent of lateral spread of isobars for the footings F1 and F2. Further, the displacement contours extend to a greater depth in case of footing F2 in comparison to footing F1 indicating higher bearing capacity for the former. Similar trend was observed from Fig. 10(iii) and Fig.10 (iv). Furthermore, study of Fig.10 (v) and Fig.10 (vi) reveals that displacement contours extend to the ground surface but the maximum displacement was observed beneath the base of the footing. From the study of Fig. 10(vii) to Fig.10(x), it was observed that the

displacement contours intercepted and confined below the base of footings F1 and F2 resulting increase in the bearing capacity. This can be due to the entire contribution of the lower dense sand layer towards the increase in the bearing capacity. Similar trend of displacement contours was observed for H/B ratio of 1 and 1.5 with the exception that the confinement of the displacement contours within sand S2 was observed beyond $D_f/B$= 1 and 1.5. The trend was similar for all the combination of friction angles of upper loose and lower dense sand layers. The insights gained from the above can be useful for developing analytical solutions for the similar problem.

### 4.5. Vectorial Displacements

Typical vectorial displacement for the footing F1 and F2 with varying $D_f/B$ ratio varying from 0 to 1.5 corresponding to H/B ratio of 0.5 and a constant friction angle of the upper loose sand (30º) and lower dense sand (40º) layer was presented in Fig. 11.

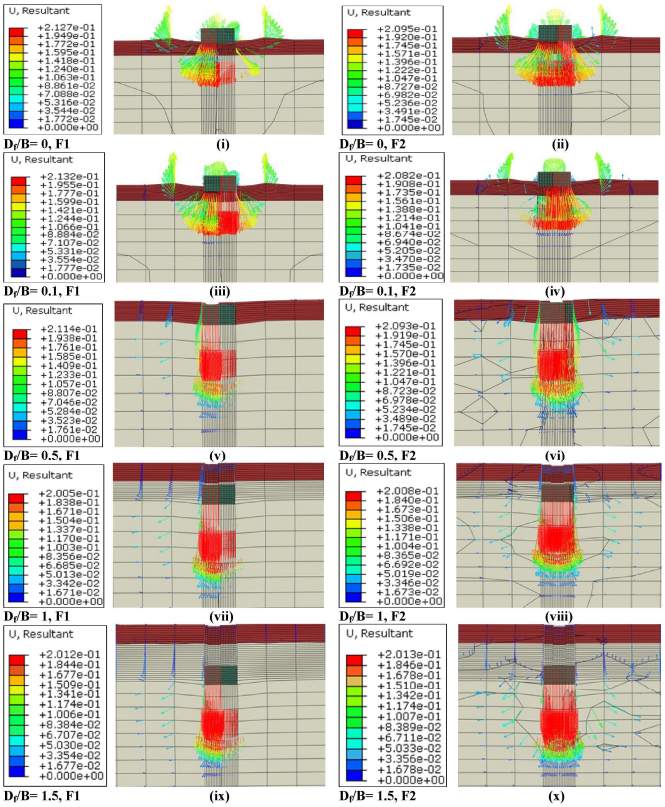


Fig. 11. Typical displacement vectors at H/B=0.5 with different $D_f/B$ ratio corresponding to $\emptyset_1 = 30°$ and $\emptyset_2 = 40°$ for footing F1 (i, iii, v, vii, ix) and F2 (ii, iv, vi, viii, x)

Study of Fig.11 reveals that there was bulging in the upper loose sand layer for $D_f/B$ = 0.1. Beyond this, no occurrence of bulging was observed. This can be attributed to the fact that the vector crossed the lower dense sand layer up to a great depth for the case with $D_f/B$ = 0.5 to 1.5. Further, from Fig.11, it was observed that as the depth of embedment increased, the extent of vertical spread of the displacement vector increased beneath the footings base indicating improvement in the bearing capacity. This trend was observed to be similar for all the combination studied.

### 4.6. Failure Pattern

Fig. 12 depicts a typical failure pattern for the footings F1 and F2 with an H/B ratio ranging from 0.5 to 1.5, corresponding to a $D_f/B$ ratio of 0.5 and a constant friction angle of the upper loose sand (34°) and lower dense sand (44°) layer.

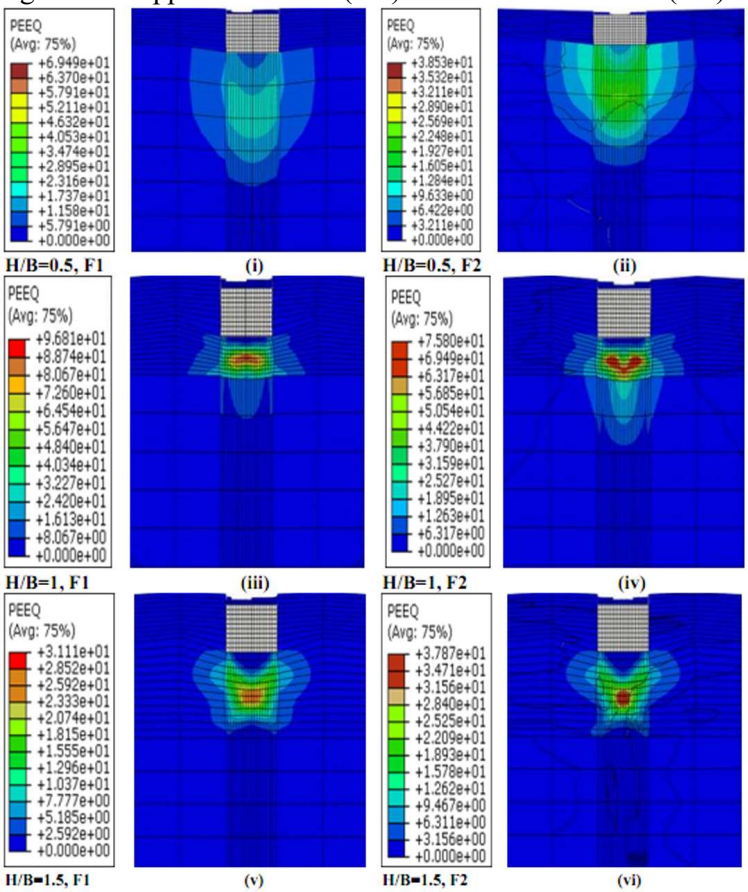


Fig. 12. Typical failure pattern at $D_f/B$=0.5 with different H/B ratio corresponding to $\emptyset_1 = 34°$ and $\emptyset_2 = 44°$ for footing F1 (i, iii, v) and F2 (ii, iv, vi)

For H/B = 0.5, the lateral extent of failure pattern was larger in case of footing F2 in comparison to footing F1 indicating higher bearing capacity for the former. With the increase in the H/B ratio to 1, the lateral and vertical extent of the failure pattern in case of footing F2 was larger in comparison to footing F1. Further, when the H/B ratio increased to 1.5 the lateral and vertical extent of the failure pattern in case of footings F2 and F1 was almost similar indicating marginal difference in the bearing capacity.

## 5. CONCLUSION

The numerical study was conducted to analyze the pressure settlement behaviour and bearing capacity of embedded asymmetric plus shaped footing on layered sand. For this purpose, the effect of variation of the friction angle of both the layers, embedment depth, and thickness of the upper loose sand were taken into consideration. The results of the numerical study were presented in a dimensionless form. From the results and discussion made above, following conclusion are put forward:

1. Significant improvement in the behaviour of footings F1 and F2 was observed with the increase in the depth of embedment and friction angle of both the sand layers.
2. For $D_f/B \geq H/B$, the pressure-settlement behaviour changed from local to general shear failure in case of footing F1.
3. The depth of embedment improved the bearing capacity and the rate of improvement was higher when $D_f/B$ lies within loose sand layer.
4. The highest increase in dimensionless bearing capacity was observed at a $D_f/B$ ratio of 1.5. The increase in the bearing capacity was 12.62 and 11.40 times with respect to the surface footing F1 and F2 corresponding to an H/B ratio of 1.5.
5. The lowest increase in the dimensionless bearing capacity was observed at $D_f/B$ ratio of 0.1 and the corresponding increase in the bearing capacity was 1.05 and 1.02 times with respect to the surface footing for footing F1 and F2 at H/B equal to 1.5
6. With increase in the H/B ratio, decrement in bearing capacity was observed. However, the rate of decrease was found to decrease with the increase in embedment depth.
7. At $D_f/B=0$, with increase in $\emptyset_1$ and $\emptyset_2$, increase in the dimensionless bearing capacity was observed. However, the effect of $\emptyset_2$ was dominant till H/B =0.5. Similarly, at $D_f/B$ =0.5, the effect of $\emptyset_2$ was dominant upto H/B =1.
8. The dimensionless bearing capacity for the footings F1 and F2 was same at H/B =0.5 with $D_f/B \geq 1$, at H/B=1 with $D_f/B \neq 0.5$ and at H/B=1.5 with $D_f/B \neq 1$.

However, using an experimental study on a similar size asymmetric embedded plus shaped footing; further confirmation of the findings reported in this paper is recommended. The proposed numerical analysis could be useful for architects working on similar superstructures that involve similar shaped footings.

## Acknowledgment
I would like to express my special gratitude to Central Building Research Institute (CSIR-CBRI) Roorkee for providing me the opportunity to utilize the ABAQUS software.

## Conflict of interest
The authors have no conflict of interest with anyone related to the material presented in the paper

**NOTATIONS**
B= Width of Footing
H= thickness of the upper loose sand
$\gamma$ = unit weight of sand
$\phi$ = internal angle of friction of sand
$\nu$ = poison's ratio
E= Modulus of Elasticity
$\Psi$ = Dilation angle
$D_f$ = depth of embedment
$q_u$ = Ultimate bearing capacity
$q_u / \gamma_1 B$ = Dimensionless ultimate bearing capacity

## REFERENCES

1. Arabpanahan, M, Mirghaderi SR, Hosseini, A, Sharif, AP and Ghalandarzadeh, A 2019. Experimental-numerical investigation of embedment effect on foundation behaviour under vertical loading, *International Journal of Civil Engineering*, **17(12)**,1951-1969.
2. Bowles, JE 1997. *Foundation Analysis and Design*, New York: McGraw-Hill Companies.
3. Dawarci, B, Ornek, M and Turedi, Y 2004. Analysis of multi-edge footing rested on loose and dense sand, *Periodica Politechnica Civil Engineering*, **58(4)**, 355-370.
4. Das, PP, Khatri, VN and Dutta, RK 2019. Bearing capacity of ring footing on weak sand layer overlying a dense sand deposit, *Geomechanics and Geoengineering*, ISNN: 1748-6025.

5. El Kasaby El-Sayed AA 1991: Estimation of guide values for the modulus of elasticity of soil, *Bulletin of Faculty of Engineering*, Assiut University, **19(1)**,1-7.
6. Ghazavi, M and Hadiani, N 2005. *Bearing capacity of multi-edge foundations*, MS thesis, Tehran (Iran): Department of civil engineering, K.N.T. university of Technology.
7. Ghazavi, M and Mokhtari, S 2008. *Numerical Investigation of Load-Settlement Characteristics of Multi-Edge Shallow Foundations*. The 12th International conference of International Association for Computer Methods and Advances in Geomechanics ( IACMAG),Goa, India,1-6 October.
8. Gnananandarao, T, Khatri, VN and Dutta, RK 2018. Pressure settlement ratio behaviour of plus shaped skirted footing on sand, Journal of Civil Engineering (IEB), **46(2)**, 161-170.
9. Hanna, AM 1982. Bearing capacity of foundations on a weak sand layer overlying a strong deposit, *Canadian Geotechnical Journal*, **19(3)**, 392-396.
10. Hazell, E 2004. *Interaction of closely spaced strip footings*. Fourth year project report, Department of engineering science, University of Oxford.
11. IS 800 2007. *Indian Standard for General Construction in Steel - Code of Practice*, New Delhi, India, Bureau of Indian Standard (Third Revision).
12. Kumar, J, Khatri, VN and Kumar, A 2020. *Performance of Skirted and Embedded Circular Footing on Sand*, Second ASCE India Conference on "Challenges of Resilient and Sustainable Infrastructure Development in Emerging Economies" (CRSIDE2020), March 2-4.
13. Meyerhof, GG and Hanna, AM 1978. Ultimate bearing capacity of foundations on layered soils under inclined load, *Canadian Geotechnical Journal*, **15(4)**, 565-572.
14. Nur, HR, Islam, MS, and Rokonuzzaman, M 2018. *The Effect of Embedment Depth on Bearing Capacity of Strip Footing in Cohesive Frictional Medium*, Proceedings of the 4th International Conference on Civil Engineering for ustainable Development (ICCESD2018), KUET, Khulna, Bangladesh ,9-11 Feb.
15. Peck, RB, Hanson, WE and Thornburn, TH 1953.*Foundation Engineering*, New York: John Wiley and sons.
16. Szypcio, Z and Dołżyk, K 2006. The bearing capacity of layered subsoil, *Studia Geotechnica et Mechanica* **28(1)**,45-60.
17. Thakur, A and Dutta, RK 2020. Experimental and numerical studies of skirted hexagonal footings on three sands," SN Applied Sciences, **2(3)**, 487.
18. Yahia-Chief, H, Mabrouki, A, Benmeddour, D and Mellas, M 2017. Bearing capacity of embedded strip footings on cohesionless soil under vertical and

horizontal loads. *Geotechnical and Geological Engineering*,**35**,547-558.
19. Zou, X, Hu, Y, Hossain, MS and Zhou, M 2018. Capacity of skirted foundation in sand-over-clay under combined V-H-M loading, *Ocean Engineering*, **159**, 201-218.

*Editor received the manuscript: 06.04.2021*